HHS Public Access

Author manuscript

Bioconjug Chem. Author manuscript; available in PMC 2020 March 02.

Published in final edited form as:

Bioconjug Chem. 2019 April 17; 30(4): 1175–1181. doi:10.1021/acs.bioconjchem.9b00118.

A Near-IR Fluorescent Dasatinib Derivative That Localizes in Cancer Cells

Syed Muhammad Usama, **Bosheng Zhao**, **Kevin Burgess***

Department of Chemistry, Texas A & M University, Box 30012, College Station, Texas 77842, United States

Abstract

Kinase inhibitors (KIs) have had a huge impact on clinical treatment of various cancers, but they are far from perfect medicines. In particular, their efficacies are limited to certain cancer types and, in many cases, provide only temporary remission. This paper explores the possibility of covalently binding a fluorophore for in vivo optical imaging to the KI dasatinib where the particular fluorophore chosen for this study, a heptamethine cyanine (Cy) derivative, tends to accumulate in tumors. Thus, we hypothesized that the dasatinib−fluorophore conjugate might target tumor cells more effectively than the parent KI, give enhanced suppression of viability, and simultaneously serve as a probe for optical imaging. As far as we are aware, the dasatinib conjugate (**1**) is the first reported to contain this KI and a probe for near-IR imaging, and it is certainly the first conjugate of a tumor-targeting near-IR dye and a KI of any kind. Conjugate 1 suppressed the viability of liver cancer cells (HepG2) more effectively than dasatinib at the same concentration. In scratch assays, 1 prevented regrowth of the tumor cells. Conjugate 1 is cell permeable, and confocal imaging indicates the fluorescence of those cells is concentrated in the mitochondria than lysosomes. In general, this study suggests there is untapped potential for conjugates of KIs with *tumor-targeting* near-IR dye and a KI of any kind. Conjugate **1** suppressed the viability of liver cancer cells (HepG2) more effectively than dasatinib at the same concentration. In scratch assays, **1** prevented regrowth of the tumor cells. Conjugate **1** is cell permeable, and confocal imaging indicates the fluorescence of those cells is concentrated in the mitochondria than lysosomes. In general, this study suggests there is untapped potential for conjugates of KIs with tumor-targeting near-IR dyes in the development of theranostics for optical imaging and treatment of cancer.

Graphical Abstract

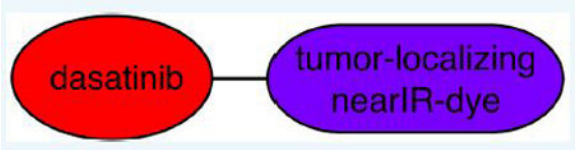

*Corresponding Author burgess@tamu.edu.

ASSOCIATED CONTENT

Supporting Information

The Supporting Information is available free of charge on the ACS Publications website at DOI: 10.1021/acs.bioconjchem.9b00118.

Synthesis scheme, characterization (NMR, HRMS), photophysical properties, in vitro assay details of 1 and supporting figures (PDF)

The authors declare no competing financial interest.

INTRODUCTION

Dasatinib (Sprycel) is a tyrosine kinase inhibitor (TKI) clinically used to treat Philadelphia chromosome, chronic myeloid leukemia, and acute lymphoblastic leukemia (https://www.cancer.gov/about-cancer/treatment/drugs). According to clinicaltrials.gov, dasatinib (alone or in combination with other chemotherapy agents) features in over 120 in clinical trials for different types of cancers, including pancreatic, nonsmall cell lung carcinoma, and bone metastases of breast cancer. However, dasatinib's efficacy is diminished by cell-efflux,[1−5] and, eventually, acquired resistance via mutations in and around the tyrosine kinase active site.

Dasatinib inhibits multiple kinases, including Bcr-Abl and members of the Src-family. While polypharmacology[6−8] is sometimes desirable, poor selectivity may lead to side effects. Indeed, dasatinib tends to reduce counts for platelets and red and white blood cells; these physiological effects may account for anemia, pulmonary edema, and heart function complications that are observed in some patients receiving this drug.[9,10]

Two strategies to increase efficacy of KIs are possible. One of these features structural modifications that reduce off-target interactions. The other focuses on conjugating the drug to agents (typically antibodies, but sometimes small molecules) that bind cell-surface receptors and enhance intracellular drug concentrations in cancer cells relative to healthy ones, increasing therapeutic indices. Research described in this paper was initiated to explore the second strategy. Additionally, we wanted to make a derivative of dasatinib that would *target cancer cells and be near-IR fluorescent.* We hypothesized that this fluorescence could be used to track the conjugate in cell studies and would have potential in theranostic applications involving optical imaging and tumor suppression *in vivo* with improved localization in cancer cells. One possibility was to conjugate a near-IR dye and a small molecule targeting group to a KI, but more compact molecular designs are preferred. The innovation in this study is to form conjugates with a special subset of heptamethine cyanine (Cy7) dyes, **A**−**C**, that are known to enhance delivery of the conjugate into solid tumors and show no systemic toxicity in mice; i.e., they are both targeting and fluorescent.[11−18]

The following text outlines some salient literature on dyes **A**−**C**. First, these water-soluble fluorophores absorb at around 780 nm with high extinction coefficients, and fluoresce at around 800 nm with acceptable quantum yields; i.e., they have excellent characteristics for optical imaging *in vivo*.[19−22] Cellular and *in vivo* studies indicate **A** localizes in many different types of cancer lines and in solid tumors (e.g., prostate,[23] gastric,[24] kidney[25]) but not in normal cells and tissue.[26−30] Preferential uptake of **A** in cancer cells is putatively mediated by Organic Anion Transporting Polypeptides (OATPs).[31,32] Specifically, hypoxia (common in solid tumors) triggers activation of HIF1α, which promotes OATP expression,[24,33] and these receptors influx organic anions and some neutral materials that are important to cell metabolism (e.g., bile salts, steroids, bilirubin, and thyroid hormones). To balance this ion influx, OATPs efflux intracellular bicarbonate,

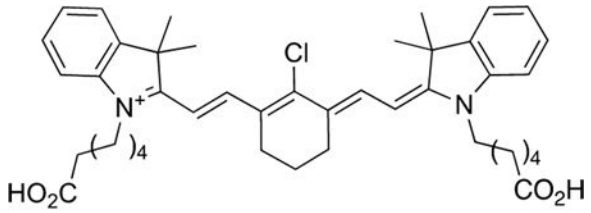

A

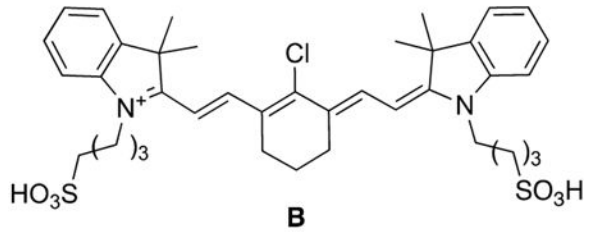

B

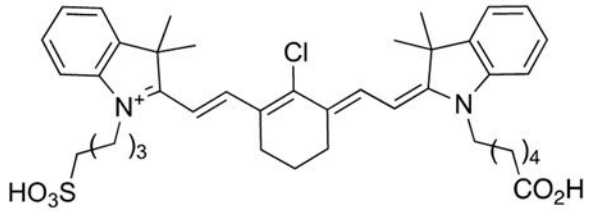

C

glutathione, and glutathione-adducts. Consequently, OATPs may promote influx of suitable small molecule organics into cancer cells, including some drug structures and the cyanine dyes **A**, **B**, and **C** shown above, *without pumping them out.*

Our group is interested in the design of small molecules that bind cell surface receptors and increase the concentration of the drug in cancerous cells, relative to healthy ones.[34–37] We saw the potential of conjugates formed by tethering cyanine dyes like **A** or **C** to kinase inhibitors (KIs) such as dasatinib. Such conjugates might be preferentially delivered into cancerous over healthy cells via the OATPs, and their desirable near-IR fluorescence properties would facilitate intracellular imaging so uptake of the conjugate could be tracked. Conversely, it was not clear that conjugate **1** would retain their inhibition activity against SRC kinases, but we estimated the probability that they would retain their activity as high enough to justify syntheses and a series of cell studies. In the event the data collected on these conjugates are interesting, those studies are reported here.

RESULTS AND DISCUSSION

Design, Synthesis, and Characteristics of Conjugate 1.

There are crystal structures of dasatinib **D** complexed with the cellular sarcoma kinase (cSrc),[38] Abelson kinase (Abl),[39] and Lck/Yes novel kinase (Lyn).[40] In these structures, the hydroxyl group of the KI projects into solvent, while the heterocyclic scaffold binds the

kinase active site (Figure 1). On the basis of this observation we hypothesized that kinase inhibitors could be added to that hydroxyl group without major perturbations to their efficacy. Consequently, we designed conjugate **1** which conjugates dasatinib to cyanine A via the solvent-exposed hydroxyl group. We hypothesized **1** might be selectively imported into cancer cells via the OATPs, and transport the kinase inhibitor fragment with it. Once inside the cell, **1**, being larger and more polar than dasatinib alone, might be less vulnerable to efflux via mechanisms featuring P-glycoprotein and alike.[1–5]

Conjugate 1 was prepared by coupling dasatinib with the parent cyanine dye in a 1:1 stoichiometry as described in the Supporting Information. In water with 0.1% Kolliphor EL (to prevent aggregation), **1** was observed to have a maximal absorbance at 796 nm, and emission at 815 nm (Figure S1). The fluorescence quantum yield of **1** (8%) and extinction coefficient of 205 480 M^{-1} cm^{-1} are typical of near-IR Cy7 dyes, hence conjugate 1 has brightness ($\Phi \times \varepsilon_{max}$) similar to that of parent dye **A**.

Cell Studies.

Cell studies were performed on HepG2 human hepatocellular carcinoma (HCC) cell line, for the following reasons. First, even though dasatinib is not approved for treatment of HCC, it is a logical therapeutic to test since signaling via the Src kinases[41] is heavily implicated in this disease.[41,42] Indeed, dasatinib has featured in cellular,[42] preclinical, and clinical trials for HCC (NCT00459108, NCT00835679, NCT00382668). Second, while noninvasive optical imaging of the liver is impractical because it is a deeply imbedded organ, surgical intervention is often practiced for advanced liver cancer, hence development of a theranostic that selectively stains cancerous tissue in a diseased liver could potentially assist excision with negative margins while simultaneously suppressing tumor growth and metastases.

KinaseSeeker assays were used to determine IC_{50} values of **1** with Src and Lyn. This is a competition binding assay in which change in luminescence signal is measured by displacement of active site displacement probe by inhibitor. Observed IC_{50} values, for **1** were 184 nM (Src) and 556 nM (Lyn), whereas the corresponding values for **D** were 12 nM (Src) and 18 nM (Lyn). Thus, conjugation of dasatinib with **A** perturbed the affinity of the kinase inhibitor part for the parent kinases, but significant binding was still observed (Figure S1b and c).

Figure 2a shows cytotoxicity data for HepG2 cells treated with **1**, **D**, **A**, and a mixture of {**A** + **D**} where the concentrations of **1**, **D**, **A**, **A**-fragment, and **D**-fragment were equal throughout. Conjugate **1** (blue line; IC_{50} 5.38 ± 0.36 μM) decreased cell viability by almost an order of magnitude relative to the parent kinase inhibitor **D** (red line; IC_{50} 34.0 ± 4.95 μM), the cyanine dye **A** (green line; IC_{50} 18.9 ± 1.35 μM), and relative to a mixture of **A** and **D** unconjugated at the same concentrations (purple line; IC_{50} 14.9 ± 0.9 μM). A cell proliferation assay was performed to determine effect of 5 μM **1**, **D**, **A**, and **A** + **D** on HepG2 cells. Compound **1** inhibited cell growth more than **D**, **A**, or **A** + **D** Figure S1d). Treatment with 1 caused the cells to change shape in the short term, and most died after 48 h, whereas those treated with the dasatinib D alone were largely unperturbed (Figure 2b). Figure 2c shows average speed of scratch closure from wound healing experiments to simulate cell

migration; DMSO (control) and **A** had comparable effects on the average speed of migration, but the rate of recovery was less in the experiments featuring **1** and **D**.

Dasatinib is designed to curb the proliferation of cancer cells, rather than be cytotoxic in the way that early cancer drugs are. In fact, the free dye **A** showed slightly *more* cytotoxicity than dasatinib (Figure 2a). Thus, beside the attributes of a near-IR labeled kinase inhibitors outlined above, for HepG2 cells there may be some toxicity of the dye itself that synergizes with the effects of the dasatinib component.

Confocal images of HepG2 cells treated with 1 indicated that the conjugate internalized more in mitochondria than lysosomes (Figure 3). The parent dye **A** also localizes in mitochondria,[23,25,26] hence this data indicates **1** is imported by the same mechanism, or that the link is broken in cells to liberate the free dye. Localization in mitochondria is characteristic of lipophilic, positively charged, organic materials, like **A**. Moreover, import through OATPs receptors is often associated more with localization in the mitochondria than endocytosis.[30]

A series of experiments were undertaken to determine the mechanism of uptake of **1** into HepG2 cells. Figure 4a shows the fluorescence of cells incubated with **1** for 30 min, washed, then visualized under a 775/46 nm filter (710/40 nm excitation); this experiment provides a calibration point for subsequent ones in the same figure, in which uptake through the OATPs is blocked, or their expression is enhanced. Significantly less fluorescence uptake was observed when the experiments were repeated under exactly the same conditions except that a pan-OATP inhibitor (bromosulfophthalein, BSP)[43] was included in the medium (Figure 4b). Conversely, the near-IR fluorescence of the cells was significantly *increased* if DMOG (dimethyloxalylglycine),[44,45] an inducer of hypoxia, was added to the medium instead. OATP uptake is energy dependent (ATP mediated), hence it shuts down after incubation at low temperatures.[46] Thus, in the light of the data above, it is unsurprising that uptake of the near-IR fluorescence was suppressed when the cells were incubated at 0 °C (Figure S3). Figure 4d shows quantitation of this data via flow cytometry. However, these experiments are only indicative, they do not prove OATP uptake is operative; elucidation of the mechanism(s) of uptake is an ongoing area of investigation in our laboratory.

Finally, induction of intracellular Src phosphorylation was probed in a blotting assay. HepG2 cells were incubated with **1**, **D**, **A** for 24 h before lysis. Total cell lysates were calibrated and subjected to SDS-PAGE followed by blotting with mAbs. **1** was shown to inhibit phosphorylation of Src family kinases in a dose-dependent way, though not as effectively as **D**. Dye **A** does not inhibit Src phosphorylation (Figure 5).

CONCLUSIONS

To date there are eight papers that feature conjugates of **A** with cytotoxic materials which preserve the *meso*-chloride functionality. These include two different experimental monoamine oxidase inhibitors,[11–14] an experimental faresnyl transferase inhibitor,[15] a mustard agent[16] and gemicitabine.[17,18] However, there are no reports of conjugation of **A** or relevant analogs to *kinase inhibitors*. The therapeutic window for kinase inhibitors is

arguably wider that for conventional cytotoxic drugs. Consequently, the merits of active targeting are perhaps less obvious for kinase inhibitors than for generally cytotoxic materials. However, we believe the prospect of cyanine−drug conjugates binding to albumin, permeating into the tumor, then *being retained there as an albumin complex* is an exciting possibility with respect to potential therapeutic applications.

Kinase inhibitors have problems associated with efflux from cells[47−50] and acquired resistance.[51] Consequently, they may be less susceptible to these undesirable characteristics because they become covalently bound to kinases are now highly topical.[52−55] We see a complementary potential here since conjugate **1** is actively imported into cells and the fluorescence is retained in cells for at least 24 h. These data indicate that **1** either dasatinib must be cleaved from **1** to be active, or **1** can inhibit phosphorylation by SRC kinases, but less effectively than dasatinib itself. We think the data in Figure 5 indicating **1** has a *greater* effect on cell viability may be attributable to the conjugate being retained in cells for longer than the parent inhibitor, perhaps circumventing efflux mechanisms that expel dasatinib form the cells. It is also possible that the inhibitor is more effective because the fluorophore directs it to the mitochondria. An alternative explanation, that the conjugate has a greater effect on other kinases, seems much less likely.

Conjugate **1** is based on near-IR dyes in the series **A**−**C**; these dyes are known to localize in *many* different solid tumors (e.g., prostate,[23] gastric,[24] kidney[25]). Consequently, research described in this paper highlights opportunities for testing conjugates of other kinase inhibitors with tumor-targeting cyanine dyes in models for other types of cancers.

Supplementary Material

Refer to Web version on PubMed Central for supplementary material.

ACKNOWLEDGMENTS

A patent application on conjugates of the kind described has been filed through Small Molecule PPI inhibitors PLC with the permission of TAMU. We thank DoD BCRP Breakthrough Award (BC141561), CPRIT (RP150559 and RP170144), and The Robert A. Welch Foundation (A-1121), Texas A&M University (RP180875) and NSF (M1603497) for financial support. The NMR instrumentation at Texas A&M University was supported by a grant from the National Science Foundation (DBI-9970232) and the Texas A&M University System. The use of the Microscopy and Imaging Center facility at Texas A&M University is acknowledged. The Olympus FV1000 confocal microscope acquisition was supported by the Office of the Vice President for Research at Texas A&M University. The use of Chemistry Mass Spectrometry Facility is acknowledged.

REFERENCES

(1). Chen Y, Agarwal S, Shaik NM, Chen C, Yang Z, and Elmquist WF (2009) P-glycoprotein and breast cancer resistance protein influence brain distribution of dasatinib. J. Pharmacol. Exp. Ther. 330, 956–963. [PubMed: 19491323]

(2). Lagas JS, van Waterschoot RAB, van Tilburg VACJ, Hillebrand MJ, Lankheet N, Rosing H, Beijnen JH, and Schinkel AH (2009) Brain Accumulation of Dasatinib Is Restricted by P-Glycoprotein (ABCB1) and Breast Cancer Resistance Protein (ABCG2) and Can Be Enhanced by Elacridar Treatment. Clin. Cancer Res. 15, 2344–2351. [PubMed: 19276246]

(3). Agarwal S, Mittapalli RK, Zellmer DM, Gallardo JL, Donelson R, Seiler C, Decker SA, SantaCruz KS, Pokorny JL, Sarkaria JN, et al. (2012) Active Efflux of Dasatinib from the Brain Limits

Efficacy against Murine Glioblastoma: Broad Implications for the Clinical Use of Molecularly Targeted Agents. Mol. Cancer Ther. 11, 2183–2192. [PubMed: 22891038]

(4). Schiff D, and Sarkaria J (2015) Dasatinib in recurrent glioblastoma: failure as a teacher. Neuro. Oncol. 17, 910–1. [PubMed: 25964312]

(5). De Witt Hamer PC (2010) Small molecule kinase inhibitors in glioblastoma: a systematic review of clinical studies. Neuro-Oncology 12, 304–316. [PubMed: 20167819]

(6). Peters J-U (2013) Polypharmacology - Foe or Friend? J. Med. Chem. 56, 8955–8971. [PubMed: 23919353]

(7). Reddy AS, and Zhang S (2013) Polypharmacology: drug discovery for the future. Expert Rev. Clin. Pharmacol. 6, 41–47.

(8). Anighoro A, Bajorath J, and Rastelli G (2014) Polypharmacology: Challenges and Opportunities in Drug Discovery. J. Med. Chem. 57, 7874–7887. [PubMed: 24946140]

(9). Wong S-F (2009) New dosing schedules of dasatinib for CML and adverse event management. J. Hematol. Oncol. 2, 1. [PubMed: 19149899]

(10). Conchon M, de Moura Freitas CMB, Rego M. A. d. C., and Braga Junior JWR (2011) Dasatinib - clinical trials and management of adverse events in imatinib resistant/intolerant chronic myeloid leukemia. Rev. Bras Hematol Hemoter 33, 131–9. [PubMed: 23284261]

(11). Wu JB, Lin T-P, Gallagher JD, Kushal S, Chung LWK, Zhau HE, Olenyuk BZ, and Shih JC (2015) Monoamine Oxidase A Inhibitor-Near-Infrared Dye Conjugate Reduces Prostate Tumor Growth. J. Am. Chem. Soc. 137, 2366–2374. [PubMed: 25585152]

(12). Kushal S, Wang W, Vaikari VP, Kota R, Chen K, Yeh TS, Jhaveri N, Groshen SL, Olenyuk BZ, Chen TC, et al. (2016) Monoamine oxidase A (MAO A) inhibitors decrease glioma progression. Oncotarget 7, 13842−13853.

(13). Lv Q, Yang X, Wang M, Yang J, Qin Z, Kan Q, Zhang H, Wang Y, Wang D, and He Z (2018) Mitochondria-targeted prostate cancer therapy using a near-infrared fluorescence dye-monoamine oxidase A inhibitor conjugate. J. Controlled Release 279, 234–242.

(14). Lv Q, Wang D, Yang Z, Yang J, Zhang R, Yang X, Wang M, and Wang Y (2019) Repurposing antitubercular agent isoniazid for treatment of prostate cancer. Biomater. Sci. 7, 296–306.

(15). Guan Y, Zhang Y, Xiao L, Li J, Wang J. p., Chordia MD, Liu Z-Q, Chung LWK, Yue W, and Pan D (2017) Improving Therapeutic Potential of Farnesylthiosalicylic Acid: Tumor Specific Delivery via Conjugation with Heptamethine Cyanine Dye. Mol. Pharmaceutics 14, 1–13.

(16). Zhang E, Luo S, Tan X, and Shi C (2014) Mechanistic study of IR-780 dye as a potential tumor targeting and drug delivery agent. Biomaterials 35, 771–778. [PubMed: 24148240]

(17). Wu JB, Shi C, Chu GC-Y, Xu Q, Zhang Y, Li Q, Yu JS, Zhau HE, and Chung LWK (2015) Near-Infrared Fluorescence Heptamethine Carbocyanine Dyes Mediate Imaging and Targeted Drug Delivery for Human Brain Tumor. Biomaterials 67, 1–10. [PubMed: 26197410]

(18). An J, Zhao N, Zhang C, Zhao Y, Tan D, Zhao Y, Bai B, Zhang H, Shi C, An J, et al. (2017) Heptamethine Carbocyanine DZ-1 Dye for Near-Infrared Fluorescence Imaging of Hepatocellular Carcinoma. Oncotarget 8, 56880−56892.

(19). Ethirajan M, Chen Y, Joshi P, and Pandey RK (2011) The Role of Porphyrin Chemistry in Tumor Imaging and Photodynamic Therapy. Chem. Soc. Rev. 40, 340–362. [PubMed: 20694259]

(20). Vahrmeijer AL, Hutteman M, van der Vorst JR, van de Velde CJH, and Frangioni JV (2013) Image-guided cancer surgery using near-infrared fluorescence. Nat. Rev. Clin. Oncol. 10, 507–518. [PubMed: 23881033]

(21). Frangioni JV (2003) In vivo near-infrared fluorescence imaging. Curr. Opin. Chem. Biol. 7, 626–634. [PubMed: 14580568]

(22). Hilderbrand SA, and Weissleder R (2010) Near-infrared fluorescence: application to in vivo molecular imaging. Curr. Opin. Chem. Biol. 14, 71–79. [PubMed: 19879798]

(23). Yuan J, Yi X, Yan F, Wang F, Qin W, Wu G, Yang X, Shao C, and Chung LWK (2015) Near-Infrared Fluorescence Imaging of Prostate Cancer Using Heptamethine Carbocyanine Dyes. Mol. Med. Rep. 11, 821–828. [PubMed: 25354708]

(24). Zhao N, Zhang C, Zhao Y, Bai B, An J, Zhang H, Shi C, and Wu Jason B (2016) Optical Imaging of Gastric Cancer With Near-Infrared Heptamethine Carbocyanine Fluorescence Dyes. Oncotarget 7, 57277−57289.

(25). Yang X, Shao C, Wang R, Chu C-Y, Hu P, Master V, Osunkoya AO, Kim HL, Zhau HE, and Chung LWK (2013) Optical Imaging of Kidney Cancer with Novel Near Infrared Heptamethine Carbocyanine Fluorescent Dyes. J. Urol. 189, 702–710. [PubMed: 23000848]

(26). Yang X., Shi C., Tong R., Qian W., Zhau HE., Wang R., Zhu G., Cheng J., Yang VW., Cheng T., et al. (2010) Near IR Heptamethine Cyanine Dye-Mediated Cancer Imaging. Clin. Cancer Res. 16, 2833–2844. [PubMed: 20410058]

(27). Zhang C, Liu T, Su Y, Luo S, Zhu Y, Tan X, Fan S, Zhang L, Zhou Y, Cheng T, et al. (2010) A near-infrared fluorescent heptamethine indocyanine dye with preferential tumor accumulation for in vivo imaging. Biomaterials 31, 6612–6617. [PubMed: 20542559]

(28). Luo S, Yang X, and Shi C (2016) Newly Emerging Theranostic Agents for Simultaneous Cancer targeted Imaging and Therapy. Curr. Med. Chem. 23, 483–497. [PubMed: 26695513]

(29). Gao M, Yu F, Lv C, Choo J, and Chen L (2017) Fluorescent chemical probes for accurate tumor diagnosis and targeting therapy. Chem. Soc. Rev. 46, 2237–2271. [PubMed: 28319221]

(30). Tan X, Luo S, Wang D, Su Y, Cheng T, and Shi C (2012) A NIR Heptamethine Dye With Intrinsic Cancer Targeting, Imaging and Photosensitizing Properties. Biomaterials 33, 2230–2239. [PubMed: 22182749]

(31). Thakkar N, Lockhart AC, and Lee W (2015) Role of Organic Anion-Transporting Polypeptides (OATPs) in Cancer Therapy. AAPS J. 17, 535–545. [PubMed: 25735612]

(32). Kotsampasakou E, and Ecker GF (2017) Organic Anion Transporting Polypeptides as Drug Targets, in Transporters as Drug Targets (Sitte HH, Ecker GF, Mannhold R, Buschmann H, and Clausen RP, Eds.) pp 271–324, Wiley - VCH Verlag GmbH & Co. KGaA.

(33). Wu JB, Shao C, Li X, Shi C, Li Q, Hu P, Chen Y-T, Dou X, Sahu D, Li W, et al. (2014) Near-infrared fluorescence imaging of cancer mediated by tumor hypoxia and HIF1α/OATPs signaling axis. Biomaterials 35, 8175–8185. [PubMed: 24957295]

(34). Kamkaew A, Li F, Li Z, and Burgess K (2017) An agent for optical imaging of TrkC-expressing, breast cancer. MedChemComm 8, 1946–1952. [PubMed: 30108715]

(35). Kamkaew A, Fu N, Cai W, and Burgess K (2017) Novel Small Molecule Probes for Metastic Melanoma. ACS Med. Chem. Lett. 8, 179–184.

(36). Voon SH, Tiew SX, Kue CS, Lee HB, Kiew LV, Misran M, Kamkaew A, Burgess K, and Chung LY (2016) Chitosan-Coated Poly(lactic-co-glycolic-acid)-Diiodinated Boron-Dipyrromethene Nanoparticles Improve Tumor Selectivity and Stealth Properties in Photodynamic Cancer Therapy. J. Biomed. Nanotechnol. 12, 1431–1452. [PubMed: 29336539]

(37). Kue SC, Kamkaew A, Lee HB, Chung LL, Kiew LV, and Burgess K (2015) Targeted PDT Agent Eradicates TrkC Expressing Tumors Via Photodynamic Therapy (PDT). Mol. Pharmaceutics 12, 212–222.

(38). Getlik M, Gruetter C, Simard JR, Kluter S, Rabiller M, Rode HB, Robubi A, and Rauh D (2009) Hybrid Compound Design To Overcome the Gatekeeper T338M Mutation in cSrc. J. Med. Chem. 52, 3915–3926. [PubMed: 19462975]

(39). Tokarski JS, Newitt JA, Chang CYJ, Cheng JD, Wittekind M, Kiefer SE, Kish K, Lee FYF, Borzillerri R, Lombardo LJ, et al. (2006) The Structure of Dasatinib (BMS354825) Bound to Activated ABL Kinase Domain Elucidates Its Inhibitory Activity against Imatinib-Resistant ABL Mutants. Cancer Res. 66, 5790–5797. [PubMed: 16740718]

(40). Williams NK, Lucet IS, Klinken SP, Ingley E, and Rossjohn J (2009) Crystal Structures of the Lyn Protein Tyrosine Kinase Domain in Its Apo- and Inhibitor-bound State. J. Biol. Chem. 284, 284–291. [PubMed: 18984583]

(41). Chang AY, and Wang M (2013) Molecular mechanisms of action and potential biomarkers of growth inhibition of dasatinib (BMS-354825) on hepatocellular carcinoma cells. BMC Cancer 13, 267. [PubMed: 23721490]

(42). Finn RS, Aleshin A, Dering J, Yang P, Ginther C, Desai A, Zhao D, von Euw E, Busuttil RW, and Slamon DJ (2013) Molecular subtype and response to dasatinib, an Src/Abl small molecule kinase inhibitor, in hepatocellular carcinoma cell lines in vitro. Hepatology 57, 1838–1846. [PubMed: 23299860]

(43). Kullak-Ublick G-A, Hagenbuch B, Stieger B, Wolkoff AW, and Meier PJ (1994) Functional characterization of the basolateral rat liver organic anion transporting polypeptide. Hepatology 20, 411–16. [PubMed: 8045503]

(44). Jaakkola P, Mole DR, Tian Y-M, Wilson MI, Gielbert J, Gaskell SJ, von Kriegsheim A, Hebestreit HF, Mukherji M, Schofield CJ, et al. (2001) Targeting of HIF-α to the von HippelLindau ubiquitylation complex by O2-regulated prolyl hydroxylation. Science 292, 468–472. [PubMed: 11292861]

(45). Milkiewicz M, Pugh CW, and Egginton S (2004) Inhibition of endogenous HIF inactivation induces angiogenesis in ischemic skeletal muscles of mice. J. Physiol. 560, 21–26. [PubMed: 15319416]

(46). Choy CJ, Ling X, Geruntho JJ, Beyer SK, Latoche JD, Langton-Webster B, Anderson CJ, and Berkman CE (2017) (177)Lu-Labeled Phosphoramidate-Based PSMA Inhibitors: The Effect of an Albumin Binder on Biodistribution and Therapeutic Efficacy in Prostate Tumor-Bearing Mice. Theranostics 7, 1928–1939. [PubMed: 28638478]

(47). Huang W-C, Hsieh Y-L, Hung C-M, Chien P-H, Chien Y-F, Chen L-C, Tu C-Y, Chen C-H, Hsu S-C, Lin Y-M, et al. (2013) BCRP/ABCG2 inhibition sensitizes hepatocellular carcinoma cells to sorafenib. PLoS One 8, e83627/1−e83627/7.

(48). Shao J, Markowitz JS, Bei D, and An G (2014) Enzyme-and Transporter-Mediated Drug Interactions with Small Molecule Tyrosine Kinase Inhibitors. J. Pharm. Sci. 103, 3810–3833. [PubMed: 25308414]

(49). D'Cunha R, Bae S, Murry DJ, and An G (2016) TKI combination therapy: strategy to enhance dasatinib uptake by inhibiting Pgp- and BCRP-mediated efflux. Biopharm. Drug Dispos. 37, 397–408. [PubMed: 27418107]

(50). Deng J, Shao J, Markowitz JS, and An G (2014) ABC Transporters in Multi-Drug Resistance and ADME-Tox of Small Molecule Tyrosine Kinase Inhibitors. Pharm. Res. 31, 2237–2255. [PubMed: 24842659]

(51). Engel J, Lategahn J, and Rauh D (2016) Hope and Disappointment: Covalent Inhibitors to Overcome Drug Resistance in Non-Small Cell Lung Cancer. ACS Med. Chem. Lett. 7, 2–5.

(52). Kwarcinski FE, Fox CC, Steffey ME, and Soellner MB (2012) Irreversible Inhibitors of c-Src Kinase That Target a Nonconserved Cysteine. ACS Chem. Biol. 7, 1910–1917. [PubMed: 22928736]

(53). Gonzalez-Bello C (2016) Designing Irreversible Inhibitors Worth the Effort? ChemMedChem 11, 22–30. [PubMed: 26593241]

(54). Weisner J, Gontla R, van der Westhuizen L, Oeck S, Ketzer J, Janning P, Richters A, Muehlenberg T, Fang Z, Taher A, et al. (2015) Covalent-Allosteric Kinase Inhibitors. Angew. Chem., Int. Ed. 54, 10313−10316.

(55). Wu P, Clausen MH, and Nielsen TE (2015) Allosteric small-molecule kinase inhibitors. Pharmacol. Ther. 156, 59–68. [PubMed: 26478442]

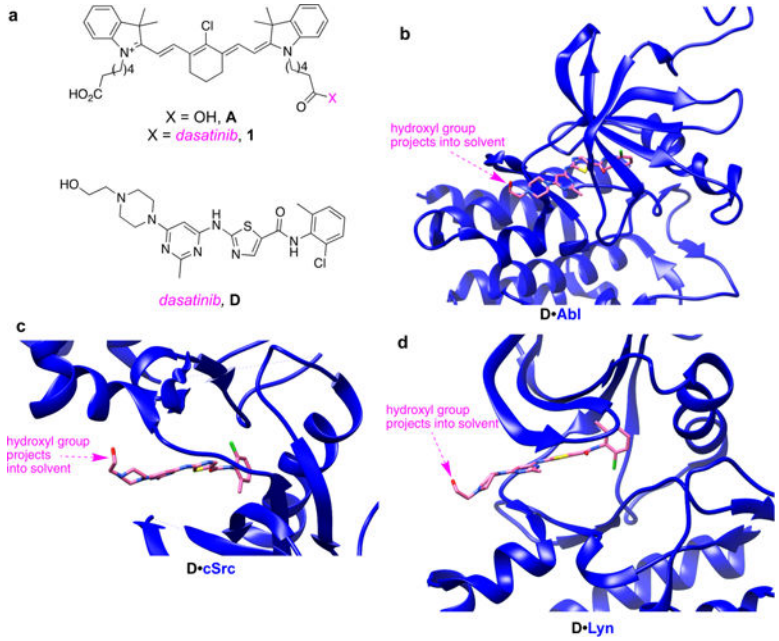

Figure 1.

a. Structure of dasatinib **D** and the KI-Cy **1**. Crystal structures of **D** bound to three of its target kinases, b, to Abl (PDB: 2GQG); c, to cSrc (3G5D); and d, to Lyn (2ZVA). All three structures show that the hydroxy group of **D** is solvent exposed.

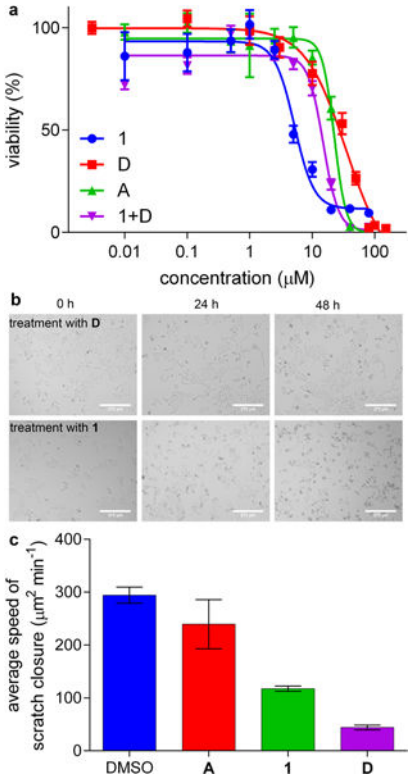

Figure 2.

a. Viabilities of HepG2 cells induced by **1**, **D**, **A**, and {**A** + **D**} after incubating with the test compounds for 48 h in the dark, before an AlamarBlue test for cell viability. b. Morphology of HepG2 cells at 10×/0.4 treated with 5 μM of **A** and **1**. c. Influence of DMSO (blank), **A**, **1**, **D** at 1 μM on a wound healing assay featuring HepG2 cells.

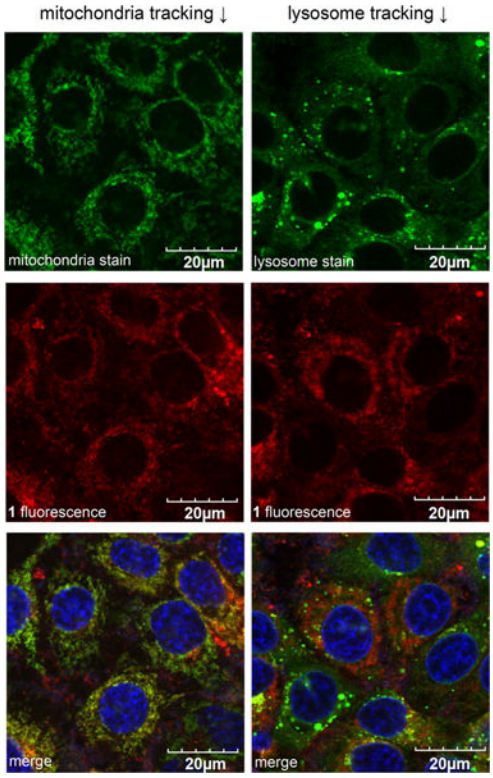

Figure 3.

Confocal imaging of HepG2 cells treated with **1** and MitoTracker Green, Pearson's coefficient 0.72 (left column) or **1** and LysoTracker Green, Pearson's coefficient 0.56 (right). Nuclei stained with NucBlue are included in the merged images in the bottom row. The images were taken at 60×/1.20 water immersed objective.

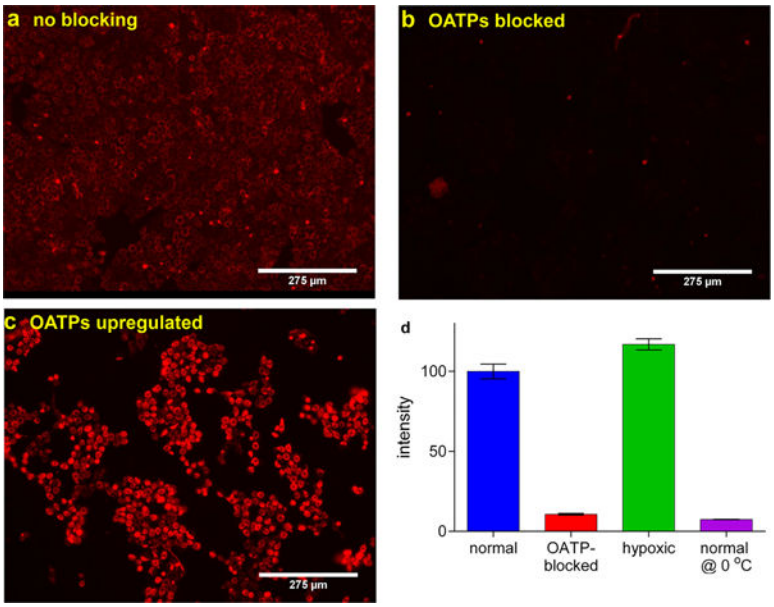

Figure 4.

Uptake of **1** under: a, normal conditions; b, in the presence of the pan-OATP inhibitor BSP (250 μM); c, under hypoxia conditions induced by 1 mM DMOG; d, quantification via flow cytometry, and scale bar 275 μm, throughout.

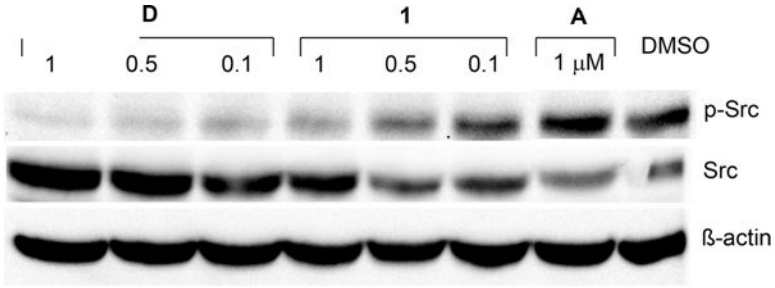

Figure 5.

Western blot analysis of HepG2 cell lysates treated with **1**, **D**, and **A**. Total protein calibrated by BCA protein assay.